HHS Public Access

Author manuscript

Int J Cardiovasc Imaging. Author manuscript; available in PMC 2017 October 01.

Published in final edited form as:

Int J Cardiovasc Imaging. 2016 October ; 32(10): 1529–1541. doi:10.1007/s10554-016-0938-5.

Comparison of 4D flow and 2D velocity-encoded phase contrast MRI sequences for the evaluation of aortic hemodynamics

Emilie Bollache[1], **Pim van Ooij**[1], **Alex Powell**[1], **James Carr**[1], **Michael Markl**[1,2], and **Alex J. Barker**[1]

Emilie Bollache: emilie.bollache@northwestern.edu

[1]Department of Radiology, Feinberg School of Medicine, Northwestern University, 737 N Michigan ave-Suite 1600, Chicago, IL 60611, USA

[2]Department of Biomedical Engineering, McCormick School of Engineering, Northwestern University, Chicago, IL, USA

Abstract

The purpose of this study was to compare aortic flow and velocity quantification using 4D flow MRI and 2D CINE phase-contrast (PC)-MRI with either one-directional (2D-1dir) or three-directional (2D-3dir) velocity encoding. 15 healthy volunteers (51 ± 19 years) underwent MRI including (1) breath-holding 2D-1dir and (2) free breathing 2D-3dir PC-MRI in planes orthogonal to the ascending (AA) and descending (DA) aorta, as well as (3) free breathing 4D flow MRI with full thoracic aorta coverage. Flow quantification included the co-registration of the 2D PC acquisition planes with 4D flow MRI data, AA and DA segmentation, and calculation of AA and DA peak systolic velocity, peak flow and net flow volume for all sequences. Additionally, the 2D-3dir velocity taking into account the through-plane component only was used to obtain results analogous to a free breathing 2D-1dir acquisition. Good agreement was found between 4D flow and 2D-3dir peak velocity (differences = −3 to 6 %), peak flow (−7 %) and net volume (−14 to −9 %). In contrast, breath-holding 2D-1dir measurements exhibited indices significantly lower than free breathing 2D-3dir and 2D-1dir (differences = −35 to −7 %, $p < 0.05$). Finally, high correlations ($r \geq 0.97$) were obtained for indices estimated with or without eddy current correction, with the lowest correlation observed for net volume. 4D flow and 2D-3dir aortic hemodynamic indices were in concordance. However, differences between respiration state and 2D-1dir and 2D-3dir measurements indicate that reference values should be established according to the PC-MRI sequence, especially for the widely used net flow (e.g. stroke volume in the AA).

Keywords

MRI; Phase-contrast; Aortic hemodynamics; 4D flow MRI

Compliance with ethical standards

Conflict of interest

None.

Introduction

The evaluation of cardiovascular hemodynamics is crucial for diagnosis and management of patients with valvular anomalies [1], congenital heart disease [2] as well as cardiomyopathies [1]. Time-resolved (CINE) phase-contrast (PC) MRI sequences, in which velocity is encoded in one direction through a 2D plane (2D-1dir) are used in clinical routine, usually during breath-holding, for quantifying blood flow and peak flow velocities [3]. However, placement of the acquisition plane remains challenging, and can lead to the underestimation of peak velocities if misplaced or not orthogonal to the flow of interest. This is a common occurrence in cases involving complex flow and where changes in flow direction occur throughout the cardiac cycle, such as with valvular stenosis, valvular regurgitation, or complex congenital heart disease. These underestimations can be improved by taking into account all flow directions, which is achieved by three-directional encoding of all three principal velocity directions inside a slice of interest (2D-3dir) [4]. Alternatively, 4D flow MRI (3D CINE PC-MRI with three-directional velocity encoding) enables post-hoc time-resolved three-dimensional visualization of blood flow and retrospective quantification at any location in a 3D volume [5]. The usefulness of the technique has been increasingly demonstrated for the assessment of blood flow hemodynamics in diverse cardiovascular territories such as the aorta [6], ventricles [7], atria [8], pulmonary arteries [9], intracranial arteries [10], portal [11] and splanchnic arteries [12].

Several previous works have focused on the comparison of 2D and 4D flow MRI for flow quantification, involving in vitro experiments [13] and in vivo in healthy subjects [13–22] or patients with congenital heart disease [17, 20, 22–24], dilated cardiomyopathy [15], valve stenosis [18], suspected intracardiac shunts [25], and other miscellaneous populations [26]. However, in these latter studies, either 2D-1dir or 2D-3dir measurements were used. In addition, the studied indices were either velocity, peak flow or flow volume. Our aim in this study is to investigate the effect of encoding 1 vs. 3 velocity directions and of acquiring data through a 2D plane vs. a 3D volume, by reporting a systematic and comprehensive comparison of 2D-1dir, 2D-3dir and 4D flow MRI for the quantification of peak systolic velocity, peak flow as well as net flow volume in the ascending (AA) and descending (DA) aorta in healthy subjects. Finally, the impact of eddy current correction, as proposed by Walker et al. [27], was assessed for the estimation of each hemodynamic parameter.

Materials and methods

Population

Sixteen healthy volunteers [age 51 ± 18 (19–78) years; 11 men] with no history of cardiovascular disease were recruited between March and May 2014, with the approval of Northwestern University institutional review board and informed consent. Each subject underwent an MRI exam, which included acquisition of velocity-encoded data in the thoracic aorta using 3 sequences (2D-1dir, 2D-3dir, 4D flow MRI). All studies were performed in the morning between 7:30 and 10am after fasting and the instruction to avoid caffeine. Weight was recorded before the exam and brachial blood pressures monitored in real time and recorded every 10 min during the exam.

MRI acquisition protocol

Aortic PC-MRI data were acquired for each subject on a 1.5T MAGNETOM Aera scanner (Siemens Medical Systems, Erlangen, Germany), without the use of any contrast agent, using the three following techniques:

1. One-directional velocity encoding in the through-plane direction with a 2D CINE PC-MRI sequence (2D-1dir) during breath-holding at end-expiration, in an axial slice placed perpendicular to the mid-AA, at the level of the right pulmonary artery center.
2. Three-directional velocity encoding using a 2D CINE PC-MRI sequence (2D-3dir) during free breathing, at the same location as for 2D-1dir measurements.
3. Three-directional velocity encoding using a 4D flow PC-MRI sequence during free breathing, in a sagittal oblique volume which included the thoracic aorta (number of slices = 24–30).

Acquisitions were not performed in the same order for all subjects in order to avoid potential effects such as a decrease in heart rate and cardiac output with scan time as they lie in the magnet. For all acquisitions, prospective ECG gating with a similar covered fraction (~80 %) of the cardiac cycle, as well as segmented k-space, were used. Acquisition parameters are provided in Table 1. Respiration navigator gating was used for acquisition of 4D flow and 2D-3dir data, while positioning the acceptance window at the end-expiration phase with an efficiency of 80 %, which was previously shown to correct for respiratory motion while providing the best trade-off between scan time and measurement of peak systolic maximal velocity magnitude when compared to other schemes [28]. Of note, our 4D flow protocol is in agreement with the 4D flow consensus statement [29].

MRI data analysis

The data analysis workflow is schematically illustrated in Fig. 1. For each subject, the three acquired datasets (2D-1dir, 2D-3dir, 4D flow MRI) were preprocessed (Fig. 1a) using a tool programmed in Matlab (The Mathworks, USA) which was previously described [30]. Preprocessing included the suppression of noise by masking pixels with a low magnitude signal intensity and also those with a high velocity standard deviation throughout the cardiac cycle [27]. Then, an automated unwrapping filter was applied to correct for velocity aliasing in voxels with a velocity shift above the Venc, as compared to the velocity of spatially and temporally neighboring pixels. Finally, eddy current correction was performed by a least squares plane first-order fit to the velocity images separately for each velocity direction, applied slice by slice to static regions at end-diastole, as identified by a low velocity standard deviation across the cardiac cycle [27], while excluding areas with spatial fold-over [31]. Eddy current correction was achieved by subtracting, for each time frame, separately for each velocity direction, the fitted plane from the original velocity image.

The slice location used for 2D-1dir and 2D-3dir measurements was automatically co-registered in the thoracic aortic volume based on DICOM location and orientation information, to extract using EnSight (CEI, Apex, North Carolina, USA), at the same level

in the AA and DA and using the same orientation, 2D magnitude and velocity images from 4D flow measurements (Fig. 1b).

The next step consisted of segmenting both the AA and DA lumen borders (Fig. 1c). The segmentation was performed on 2D-1dir and 2D-3dir PC-MRI data using the Segment software version 1.9 R4040 (Medviso AB, Lund, Sweden; http://segment.heiberg.se) [32], which provided an automated time-resolved detection of aortic contours on modulus images, based on the level set method, from a manual initialization of a circular region of interest (ROI) on a single cardiac phase. A custom software [19] was used for segmentation of 2D images extracted from 4D flow data that were lower in contrast than the 2D-1dir or 2D-3dir images, which hindered the use of level set algorithms. The software allowed for manual drawing of ROI and ROI fitting based on cubic B-splines using both the magnitude and velocity images.

AA and DA systolic maximal area was extracted for 2D-1dir, 2D-3dir PC-MRI and 4D flow data. Furthermore, after applying a median filter on boundary pixels to reduce the effect of noise in velocity images, the AA and DA contours were used to estimate, for each cardiac time frame t, the following hemodynamic indices, from each sequence:

1. cross-sectionally averaged over the pixels [$Vz_{avg}(t)$] and maximal [$Vz_{max}(t)$] through-plane velocity;
2. maximal velocity magnitude $\left[\mathrm{Vmag}_{\max}(t) = \max\left(\sqrt{\mathrm{Vx}(t)^2 + \mathrm{Vy}(t)^2 + \mathrm{Vz}(t)^2}\right)\right]$;
3. flow rate [$Q(t)$ = cross-sectional area(t) × $Vz_{avg}(t)$].

Note that Vz_{max} and $Vmag_{max}$ are identical for the 2D-1dir data. Also note that the through-plane Vz_{max} estimated using the free breathing 2D-3dir data is equivalent to Vz_{max} that would be obtained using a fourth free breathing through-plane 2D-1dir sequence. The peak systolic maximal through-plane velocity (peak Vz_{max}, cm/s), peak systolic maximal velocity magnitude (peak $Vmag_{max}$, cm/s), peak systolic flow (peak Q, ml/s) and net flow volume (Q_{net}, ml), as obtained by integrating flow rate throughout systole, were further computed.

To test the effect of eddy current correction on hemodynamic measurements for each sequence, the data analysis workflow was additionally performed without correcting for eddy currents.

Statistical analysis

For global qualitative visualization and comparison, maximal through-plane velocity Vz_{max}, maximal velocity magnitude $Vmag_{max}$ and flow rate Q waveforms in the AA and DA provided by each MRI velocity-encoded sequence were interpolated using a 39 ms time step for each healthy volunteer, then averaged over the whole group and reported as mean waveforms with standard deviation bars for each cardiac time frame. Quantitative differences across the three MRI sequences at each cardiac time frame were assessed using one-way Kruskal–Wallis. Normal distribution of aortic indices was tested using the Kolmogorov–Smirnov test. AA and DA peak systolic Vz_{max} and $Vmag_{max}$, peak systolic Q,

Q_{net} volume and systolic area were reported as mean values ± standard deviations. Paired comparison between 2D-1dir and 2D-3dir as well as between 4D flow and 2D-3dir measurements was achieved using Bland–Altman analyses. Mean bias, limits of agreement, along with relative difference expressed in percentage of the mean value, were reported. Linear regression was used to study the relationship between peak Vz_{max} and $Vmag_{max}$ as well as peak Q and Q_{net}, as estimated with and without eddy current correction. Slopes, Pearson correlation coefficients r, as well as biases and limits of agreement were provided. Finally, significant differences between hemodynamic indices obtained using 2D-1dir and 2D-3dir, 4D flow and 2D-3dir, as well as with and without correcting for eddy currents, were assessed using a Wilcoxon signed-rank test. A p value <0.05 was considered as statistically significant. Statistical analyses were performed using Matlab (MathWorks, Natick, MA, USA).

Results

Population description

One female subject (6 % of the subjects) was excluded because of severe aliasing artifacts on PC-MRI data, which could not be fixed using the dedicated software nor manual correction. Mean age of the resulting 15 healthy volunteers was 51 ± 19 [19–78] years; mean weight was 192 ± 34 [130–206] lbs and systolic/diastolic blood pressures were 126 ± 25 [92–167]/76 ± 17 [30–105] mmHg.

Comparison between 2D-1dir, 2D-3dir and 4D flow MRI

Figure 2 illustrates examples of velocity profiles inside the AA and DA ROIs as obtained using 2D-1dir, 2D-3dir PC-MRI and 4D flow during systole in a healthy subject. While systolic velocity profiles look similar between 2D-3dir and 4D flow both in the AA and DA, velocities were lower when using 2D-1dir data at both locations.

Figure 3 shows maximal through-plane velocity Vz_{max}, maximal velocity magnitude $Vmag_{max}$ and flow rate Q for 2D-1dir, 2D-3dir PC-MRI and 4D flow in the AA and DA over the cardiac cycle averaged over the group of healthy volunteers. While no significant differences were observed for DA Vz_{max} and $Vmag_{max}$ as well as for AA and DA Q throughout most of cardiac phases, systolic $Vmag_{max}$ and Vz_{max} in the AA were significantly different across the three sequences. Of note, a shorter averaged systolic duration time was observed for 2D-1dir breath-hold data, when compared to 2D-3dir or 4D flow MRI data.

Results for the quantification of peak Vz_{max} and $Vmag_{max}$, peak Q, Q_{net} and systolic area in the AA and the DA for all three sequences are summarized in Table 2. We found no significant differences between 4D flow and 2D-3dir indices in the AA nor in the DA. However, both in the AA and the DA, for all parameters, the breath-hold 2D-1dir resulted in significantly reduced measurements when compared to 2D-3dir. These findings were confirmed by Bland–Altman analysis for comparisons between 2D-1dir, 2D-3dir PC-MRI and between 4D flow, 2D-3dir PC-MRI (Figs. 4, 5 respectively). Overall, mean biases, limits of agreement and relative percentage differences obtained for peak Vz_{max}, calculated when

considering only the through-plane component, were lower than those obtained for peak $Vmag_{max}$, which takes into account all three velocity components. However, peak Vz_{max} estimated using 2D-1dir data was still significantly lower than 2D-3dir peak Vz_{max} (Table 2). Note that, as expected, Vz_{max} was significantly lower than $Vmag_{max}$ when compared within the same sequence for the 2D-3dir and 4D flow measurements, both in the AA and DA ($p < 0.0005$ for all).

Effect of eddy current correction on measurement of hemodynamics indices

No significant differences were observed in peak Vz_{max} and $Vmag_{max}$ as well as peak Q and Q_{net} in neither the AA nor the DA using the three PC-MRI sequences, with or without eddy current correction ($p \geq 0.77$). Figure 6 shows the results of linear regression analysis for the comparison of hemodynamic indices with and without eddy current correction. Overall, the obtained correlation coefficients were high ($r = 0.97–0.999$, $p < 0.0001$). The lowest correlations ($r = 0.98$ and $r = 0.97$ in the AA and DA, respectively, $p < 0.0001$) were obtained when considering Q_{net}. Table 3 reports results of the Bland–Altman analysis, separately for each of the three PC-MRI sequences. The lowest biases and narrowest limits of agreement were obtained with the 2D-1dir sequence.

Table 4 summarizes findings previously reported in the literature for the comparison of flow measurements between 2D PC-MRI and 4D flow, while focusing on the aorta in healthy subjects. The corresponding findings obtained in our study are summarized at the bottom of the table for comparison.

Discussion

This is the first study systematically assessing differences in peak velocity, peak flow and volume estimated in the AA and DA of healthy volunteers, based on three flow-sensitive MRI techniques that are currently used in clinical routine and research settings. Our main findings were that: (1) breath-hold 2D-1dir measurements were significantly lower than the free breathing 2D-3dir and the synthetic free breathing 2D-1dir measurements (i.e. the through-plane ‘Vz’ velocity component extracted from the 2D-3dir data); (2) good agreement was observed for the comparison between the free breathing 2D-3dir and 4D flow sequences; (3) the highest sensitivity to eddy current correction was observed for the integrated flow indices.

Several studies previously focused on the comparison of hemodynamic indices estimated using 4D flow MRI compared to standard 2D velocity-encoded sequences [13–26]. When comparing our findings with those previously reported in the literature, focusing on proximal aorta studies including healthy volunteers (Table 4), we found that, to the best of our knowledge, only one compared 4D flow and 2D-3dir sequences. First, our AA and DA net flow volume mean values obtained using 2D-3dir and 4D flow data are within the ranges reported in this study on 19 healthy volunteers (AA 2D-3dir = 74.4 ± 16.2 ml and 4D flow = 73.9 ± 18.9 ml; DA 2D-3dir = 61.6 ± 13.0 ml and 4D flow = 45.4 ± 11.7 ml) [19]. In further concordance with this previous work [19], we found that the net volumes were lower when calculated from 4D flow than 2D-3dir data, which might be due to the lower 4D flow spatial resolution in one dimension, although the difference was not significant. Finally, the mean

absolute bias (2D-3dir − 4D flow Q_{net} = 8.88 ± 7.02 ml) and median relative difference (2D-3dir − 4D flow Q_{net} ~12 %) obtained by the authors [19] were close to ours, despite their 2D-3dir temporal resolution twice as high as their 4D flow temporal resolution. Interestingly, in our study, only four volunteers had AA 2D-3dir flow volume and peak lower than 4D flow measurements. This could be explained by the fact that, from what we observed retrospectively on 4D flow data, the 2D slice used for 2D-1dir and 2D-3dir measurements was not placed exactly orthogonal to the AA axis in these subjects (and thus partial volume effects associated with anisotropic voxels common to the 2D acquisitions may play role).

We further compared the two 2D PC-MRI sequences, and found that all 2D-1dir velocity and flow indices were significantly lower than 2D-3dir indices both in the AA and DA. The underestimation of peak velocity using a 2D through-plane velocity-encoded sequence when the acquisition plane is not positioned exactly orthogonal to the direction of flow is widely known [33], although its effect on the flow calculation should be minor. Indeed, in our study, peak through-plane velocity was significantly lower than peak velocity magnitude both estimated using the 2D-3dir data. In addition, 2D-1dir aortic peak velocity was still significantly lower than 2D-3dir peak velocity calculated while taking into account the through-plane component only, albeit to a lesser extent than when compared to 2D-3dir peak velocity magnitude calculated using the three principal components. Since data were acquired at the same location with the same slice orientation, both with prospective ECG gating and with the same range of pixel spacing, slice thickness, temporal resolution and encoding velocity, this discrepancy might be due to the differences in the employed number of segments and, importantly, in physiological conditions between acquisitions, specifically breath-holding vs. free breathing. Indeed, it was previously shown that cardiac output measured in the aorta was significantly lower during breath-holding than during free breathing [34]. This can be related to changes in systolic duration time and more generally heart rate, as previously shown between free breathing and breath-hold MRI acquisitions in patients after acute ST-segment elevation myocardial infarction [35]. In our study, we tried to avoid potential systematic changes in physiological conditions over scan time by acquiring the 3 PC MRI sequences in a different order for all subjects. Furthermore, we acquired breath-hold 2D-1dir data during end-expiration and free breathing data while positioning the respiratory navigator acceptance window at the end-expiration phase, as a recent non-electrocardiographic triggered real-time PC-MRI study further exhibited differences in flow throughout the respiratory cycle and between normal and forced breathing [36]. Of note, mean biases, limits of agreement and relative percentage differences for comparison between 2D-1dir peak through-plane velocity and 2D-3dir velocity magnitude were lower in the DA. This finding suggests that complex flow is more prominent in the AA, in agreement with previous observations [37], and highlights that in-plane velocity components should not be neglected in this region.

When referring to previous literature for the comparison between 2D-1dir and 2D-3dir measurements, we found that most studies compared 4D flow and 2D-1dir, thereby confounding the ability to understand the separate contribution of different number of velocity encoding directions and volumetric coverage. As previously reported (Table 4), we found that flow volume [14–16, 21, 25, 26] and peak flow [14] were lower and that peak

velocities were higher [18] when estimated using 4D flow in comparison with 2D measurements. Of note, our net volume measurements were lower than those previously reported both at 3T (2D-1dir = 89 ± 10 ml [18] or 100.6 ± 27.8 ml [16] and 4D flow = 88 ± 10 ml [18] or 95.9 ± 19.1 ml [16] in the AA). This could be due to the differences in the studied populations, spatial resolution and gating of MRI data, but also field strength or method used for eddy current correction. Indeed, it was previously demonstrated that flow indices estimated at 3T were higher than those estimated on a 1.5T scanner [14] that we used in our study.

The highest differences between sequences were obtained when considering the spatially integrated peak flow and especially the both spatially and temporally integrated net flow volume. This might be explained by the fact that these flow indices are very sensitive to the segmentation of aortic borders, which can prove to be challenging in cases of low contrast in the images, as is often found with 4D flow data due to the trade-off between good spatial resolution, large volume coverage and limited scan time. Indeed, a recent study focused on the effects of 4D flow MRI data segmentation methods used to calculate flow [26]. The following strategies were compared: (1) segmentation of the systolic frame only and propagation of the ROI throughout the cardiac cycle, in a single 2D slice; (2) same method 1, but averaged over 6 additional consecutive 2D slices along the aortic axis; (3) segmentation of all phases in a single slice. The authors reported that the best agreement against 2D-1dir measurements was found when using the latter method [26], which we also used in our study.

Finally, we found high correlations and low biases for the comparison of aortic indices calculated using each of the three PC-MRI sequence with and without eddy current correction. We found that ascending aortic 4D flow measurements were the most sensitive to eddy current correction, which was expected since the correction was applied slice by slice and on all three velocity components. Again, up to 10 ml differences can be obtained for net flow volume, whose high sensitivity to correction is known given its double spatially and temporally integrated feature, which confirms the need to correct for eddy currents [38].

The main limitation of our study is the lack of a true gold standard for hemodynamic measurements, which does not exist for in vivo measurements in humans. We could have considered Doppler ultrasound as a reference, although this technique provides only one-directional velocity and is highly operator-dependent. In addition, cine SSFP MRI could have been used as a gold standard for the non-invasive estimation of left ventricular stroke volume, but it was not part of the designed protocol which was focused on velocity-encoded acquisitions. However, the purpose of this study was to provide a head-to-head comparison between velocity-encoded MRI sequences, and the validation of such techniques is beyond the scope of this article. The use of prospective ECG gating could be considered as a second drawback, since it does not provide a full coverage of the cardiac cycle. It was used in our study to enable, during free breathing, the addition of a respiration navigator pulse at end-diastole. Indeed, respiration control is essential for 4D flow MRI to mitigate breathing artifacts that would otherwise cause severe ghosting or blurring, and the combination of navigator gating with retrospective ECG gating is challenging, as it would require to interrupt the data acquisition during late diastole to insert the navigator pulse and thus

forward estimation of RR-interval duration. This option was not available in our 4D flow sequence and all data were thus acquired using prospective ECG gating, including for 2D PC-MRI data in order to be consistent with 4D flow acquisition and allow for a more direct comparison between hemodynamic indices to overcome the effect of using either retrospective or prospecting gating. Quantitative comparison of velocity profiles as well as more sophisticated indices such as wall shear stress or vortices obtained using different sequences could also be studied. Another limitation is the use of two different algorithms for 2D PC-MRI and 4D flow image segmentation. However, the aortic systolic area was similar between 2D-3dir and 4D flow data, but different between 2D-3dir and 2D-1dir for which the same segmentation method was applied, probably due to different physiological conditions when acquiring data under free breathing or breath-holding. Finally, it should be underlined that the present study aimed at evaluating the effect of encoding velocity in either 1 or 3 directions and of acquiring data either in a 2D plane or in a 3D volume. To achieve this objective, we tried to match temporal and spatial resolutions between the three MRI techniques. Accordingly, different results might be obtained when using the 2D-1dir PC-MRI sequence used in clinical routine with a better achievable temporal resolution (as low as 10 ms using k-space segmentation factor = 1).

In conclusion, we found a good agreement between the two three-directional velocity-encoded sequences (differences within 10 %). However, aortic flow and velocity indices were significantly lower when measured during breath-hold than during free breathing. Differences obtained using the clinically used 2D-1dir PC-MRI sequence highlight the need to standardize acquisition protocols and to establish hemodynamic reference values specific to a given technique. In particular, care should be taken when reporting the widely used stroke volume.

Acknowledgments

Funding

This work was supported by the National Institutes of Health Grants R01HL115828 and K25HL119608.

References

1. Nishimura RA, Carabello BA. Hemodynamics in the cardiac catheterization laboratory of the 21st century. Circulation. 2012; 125(17):2138–2150. DOI: 10.1161/CIRCULATIONAHA.111.060319 [PubMed: 22547754]
2. Kappanayil M, Kannan R, Kumar RK. Understanding the physiology of complex congenital heart disease using cardiac magnetic resonance imaging. Ann Pediatr Cardiol. 2011; 4(2):177–182. DOI: 10.4103/0974-2069.84666 [PubMed: 21976882]
3. Chai P, Mohiaddin R. How we perform cardiovascular magnetic resonance flow assessment using phase-contrast velocity mapping. J Cardiovasc Magn Reson. 2005; 7(4):705–716. [PubMed: 16136862]
4. Mohiaddin RH, Yang GZ, Kilner PJ. Visualization of flow by vector analysis of multidirectional cine MR velocity mapping. J Comput Assist Tomogr. 1994; 18(3):383–392. [PubMed: 8188903]
5. Stankovic Z, Allen BD, Garcia J, Jarvis KB, Markl M. 4D flow imaging with MRI. Cardiovasc Diagn Ther. 2014; 4(2):173–192. DOI: 10.3978/j.issn.2223-3652.2014.01.02 [PubMed: 24834414]
6. Hope MD, Meadows AK, Hope TA, Ordovas KG, Reddy GP, Alley MT, Higgins CB. Images in cardiovascular medicine. Evaluation of bicuspid aortic valve and aortic coarctation with 4D flow

magnetic resonance imaging. Circulation. 2008; 117(21):2818–2819. DOI: 10.1161/CIRCULATIONAHA.107.760124 [PubMed: 18506021]

7. Toger J, Kanski M, Carlsson M, Kovacs SJ, Soderlind G, Arheden H, Heiberg E. Vortex ring formation in the left ventricle of the heart: analysis by 4D flow MRI and Lagrangian coherent structures. Ann Biomed Eng. 2012; 40(12):2652–2662. DOI: 10.1007/s10439-012-0615-3 [PubMed: 22805980]
8. Fluckiger JU, Goldberger JJ, Lee DC, Ng J, Lee R, Goyal A, Markl M. Left atrial flow velocity distribution and flow coherence using four-dimensional FLOW MRI: a pilot study investigating the impact of age and pre- and postintervention atrial fibrillation on atrial hemodynamics. J Magn Reson Imaging. 2013; 38(3):580–587. DOI: 10.1002/jmri.23994 [PubMed: 23292793]
9. Odagiri K, Inui N, Miyakawa S, Hakamata A, Wei J, Takehara Y, Sakahara H, Sugiyama M, Alley MT, Tran QK, Watanabe H. Abnormal hemodynamics in the pulmonary artery seen on time-resolved 3-dimensional phase-contrast magnetic resonance imaging (4D-flow) in a young patient with idiopathic pulmonary arterial hypertension. Circ J. 2014; 78(7):1770–1772. [PubMed: 24790032]
10. Schrauben E, Wahlin A, Ambarki K, Spaak E, Malm J, Wieben O, Eklund A. Fast 4D flow MRI intracranial segmentation and quantification in tortuous arteries. J Magn Reson Imaging. 2015; doi: 10.1002/jmri.24900
11. Roldan-Alzate A, Frydrychowicz A, Niespodzany E, Landgraf BR, Johnson KM, Wieben O, Reeder SB. In vivo validation of 4D flow MRI for assessing the hemodynamics of portal hypertension. J Magn Reson Imaging. 2013; 37(5):1100–1108. DOI: 10.1002/jmri.23906 [PubMed: 23148034]
12. Stankovic Z, Rossle M, Euringer W, Schultheiss M, Salem R, Barker A, Carr J, Langer M, Markl M, Collins JD. Effect of TIPS placement on portal and splanchnic arterial blood flow in 4-dimensional flow MRI. Eur Radiol. 2015; doi: 10.1007/s00330-015-3663-x
13. Brix L, Ringgaard S, Rasmusson A, Sorensen TS, Kim WY. Three dimensional three component whole heart cardiovascular magnetic resonance velocity mapping: comparison of flow measurements from 3D and 2D acquisitions. J Cardiovasc Magn Reson. 2009; 11:3.doi: 10.1186/1532-429X-11-3 [PubMed: 19232119]
14. Carlsson M, Toger J, Kanski M, Bloch KM, Stahlberg F, Heiberg E, Arheden H. Quantification and visualization of cardiovascular 4D velocity mapping accelerated with parallel imaging or k-t BLAST: head to head comparison and validation at 1.5T and 3T. J Cardiovasc Magn Reson. 2011; 13:55.doi: 10.1186/1532-429X-13-55 [PubMed: 21970399]
15. Eriksson J, Carlhall CJ, Dyverfeldt P, Engvall J, Bolger AF, Ebbers T. Semi-automatic quantification of 4D left ventricular blood flow. J Cardiovasc Magn Reson. 2010; 12:9.doi: 10.1186/1532-429X-12-9 [PubMed: 20152026]
16. Frydrychowicz A, Wieben O, Niespodzany E, Reeder SB, Johnson KM, Francois CJ. Quantification of thoracic blood flow using volumetric magnetic resonance imaging with radial velocity encoding: in vivo validation. Invest Radiol. 2013; 48(12):819–825. DOI: 10.1097/RLI.0b013e31829a4f2f [PubMed: 23857136]
17. Nordmeyer S, Riesenkampff E, Crelier G, Khasheei A, Schnackenburg B, Berger F, Kuehne T. Flow-sensitive four-dimensional cine magnetic resonance imaging for offline blood flow quantification in multiple vessels: a validation study. J Magn Reson Imaging. 2010; 32(3):677–683. DOI: 10.1002/jmri.22280 [PubMed: 20815066]
18. Nordmeyer S, Riesenkampff E, Messroghli D, Kropf S, Nordmeyer J, Berger F, Kuehne T. Four-dimensional velocity- encoded magnetic resonance imaging improves blood flow quantification in patients with complex accelerated flow. J Magn Reson Imaging. 2013; 37(1):208–216. DOI: 10.1002/jmri.23793 [PubMed: 22976284]
19. Stalder AF, Russe MF, Frydrychowicz A, Bock J, Hennig J, Markl M. Quantitative 2D and 3D phase contrast MRI: optimized analysis of blood flow and vessel wall parameters. Magn Reson Med. 2008; 60(5):1218–1231. DOI: 10.1002/mrm.21778 [PubMed: 18956416]
20. van der Hulst AE, Westenberg JJ, Kroft LJ, Bax JJ, Blom NA, de Roos A, Roest AA. Tetralogy of fallot: 3D velocity-encoded MR imaging for evaluation of right ventricular valve flow and diastolic function in patients after correction. Radiology. 2010; 256(3):724–734. DOI: 10.1148/radiol.10092269 [PubMed: 20634432]

21. Wentland AL, Grist TM, Wieben O. Repeatability and internal consistency of abdominal 2D and 4D phase contrast MR flow measurements. Acad Radiol. 2013; 20(6):699–704. DOI: 10.1016/j.acra.2012.12.019 [PubMed: 23510798]
22. Zaman A, Motwani M, Oliver JJ, Crelier G, Dobson LE, Higgins DM, Plein S, Greenwood JP. 3.0T, time-resolved, 3D flow-sensitive MR in the thoracic aorta: impact of k-t BLAST acceleration using 8-versus 32-channel coil arrays. J Magn Reson Imaging. 2015; 42(2):495–504. DOI: 10.1002/jmri.24814 [PubMed: 25447784]
23. Valverde I, Nordmeyer S, Uribe S, Greil G, Berger F, Kuehne T, Beerbaum P. Systemic-to-pulmonary collateral flow in patients with palliated univentricular heart physiology: measurement using cardiovascular magnetic resonance 4D velocity acquisition. J Cardiovasc Magn Reson. 2012; 14:25.doi: 10.1186/1532-429X-14-25 [PubMed: 22541134]
24. Hope MD, Meadows AK, Hope TA, Ordovas KG, Saloner D, Reddy GP, Alley MT, Higgins CB. Clinical evaluation of aortic coarctation with 4D flow MR imaging. J Magn Reson Imaging. 2010; 31(3):711–718. DOI: 10.1002/jmri.22083 [PubMed: 20187217]
25. Hanneman K, Sivagnanam M, Nguyen ET, Wald R, Greiser A, Crean AM, Ley S, Wintersperger BJ. Magnetic resonance assessment of pulmonary (QP) to systemic (QS) flows using 4D phase-contrast imaging: pilot study comparison with standard through-plane 2D phase-contrast imaging. Acad Radiol. 2014; 21(8):1002–1008. DOI: 10.1016/j.acra.2014.04.012 [PubMed: 25018072]
26. Hsiao A, Alley MT, Massaband P, Herfkens RJ, Chan FP, Vasanawala SS. Improved cardiovascular flow quantification with time-resolved volumetric phase-contrast MRI. Pediatr Radiol. 2011; 41(6):711–720. DOI: 10.1007/s00247-010-1932-z [PubMed: 21221566]
27. Walker PG, Cranney GB, Scheidegger MB, Waseleski G, Pohost GM, Yoganathan AP. Semiautomated method for noise reduction and background phase error correction in MR phase velocity data. J Magn Reson Imaging. 1993; 3(3):521–530. [PubMed: 8324312]
28. van Ooij P, Semaan E, Schnell S, Giri S, Stankovic Z, Carr J, Barker AJ, Markl M. Improved respiratory navigator gating for thoracic 4D flow MRI. Magn Reson Imaging. 2015; 33(8):992–999. DOI: 10.1016/j.mri.2015.04.008 [PubMed: 25940391]
29. Dyverfeldt P, Bissell M, Barker AJ, Bolger AF, Carlhall CJ, Ebbers T, Francios CJ, Frydrychowicz A, Geiger J, Giese D, Hope MD, Kilner PJ, Kozerke S, Myerson S, Neubauer S, Wieben O, Markl M. 4D flow cardiovascular magnetic resonance consensus statement. J Cardiovasc Magn Reson. 2015; 17(1):72.doi: 10.1186/s12968-015-0174-5 [PubMed: 26257141]
30. Schnell S, Entezari P, Mahadewia RJ, Malaisrie SC, McCarthy PM, Collins JD, Carr J, Markl M. Improved semiautomated 4D flow MRI analysis in the aorta in patients with congenital aortic valve anomalies versus tricuspid aortic valves. J Comput Assist Tomogr. 2015; doi: 10.1097/RCT.0000000000000312
31. Lankhaar JW, Hofman MB, Marcus JT, Zwanenburg JJ, Faes TJ, Vonk-Noordegraaf A. Correction of phase offset errors in main pulmonary artery flow quantification. J Magn Reson Imaging. 2005; 22(1):73–79. DOI: 10.1002/jmri.20361 [PubMed: 15971181]
32. Heiberg E, Sjogren J, Ugander M, Carlsson M, Engblom H, Arheden H. Design and validation of Segment–freely available software for cardiovascular image analysis. BMC Med Imaging. 2010; 10:1.doi: 10.1186/1471-2342-10-1 [PubMed: 20064248]
33. Lotz J, Meier C, Leppert A, Galanski M. Cardiovascular flow measurement with phase-contrast MR imaging: basic facts and implementation. Radiographics. 2002; 22(3):651–671. DOI: 10.1148/radiographics.22.3.g02ma11651 [PubMed: 12006694]
34. Sakuma H, Kawada N, Kubo H, Nishide Y, Takano K, Kato N, Takeda K. Effect of breath holding on blood flow measurement using fast velocity encoded cine MRI. Magn Reson Med. 2001; 45(2):346–348. [PubMed: 11180443]
35. Klug G, Reinstadler SJ, Feistritzer HJ, Kremser C, Schwaiger JP, Reindl M, Mair J, Muller S, Mayr A, Franz WM, Metzler B. Cardiac index after acute ST-segment elevation myocardial infarction measured with phase-contrast cardiac magnetic resonance imaging. Eur Radiol. 2016; 26(7):1999–2008. DOI: 10.1007/s00330-015-4022-7 [PubMed: 26385805]
36. Korperich H, Barth P, Gieseke J, Muller K, Burchert W, Esdorn H, Kececioglu D, Beerbaum P, Laser KT. Impact of respiration on stroke volumes in paediatric controls and in patients after Fontan procedure assessed by MR real-time phase-velocity mapping. Eur Heart J Cardiovasc Imaging. 2015; 16(2):198–209. DOI: 10.1093/ehjci/jeu179 [PubMed: 25246504]

37. Stalder AF, Frydrychowicz A, Russe MF, Korvink JG, Hennig J, Li K, Markl M. Assessment of flow instabilities in the healthy aorta using flow-sensitive MRI. J Magn Reson Imaging. 2011; 33(4):839–846. DOI: 10.1002/jmri.22512 [PubMed: 21448948]

38. Gatehouse PD, Rolf MP, Graves MJ, Hofman MB, Totman J, Werner B, Quest RA, Liu Y, von Spiczak J, Dieringer M, Firmin DN, van Rossum A, Lombardi M, Schwitter J, Schulz-Menger J, Kilner PJ. Flow measurement by cardiovascular magnetic resonance: a multi-centre multi-vendor study of background phase offset errors that can compromise the accuracy of derived regurgitant or shunt flow measurements. J Cardiovasc Magn Reson. 2010; 12:5.doi: 10.1186/1532-429X-12-5 [PubMed: 20074359]

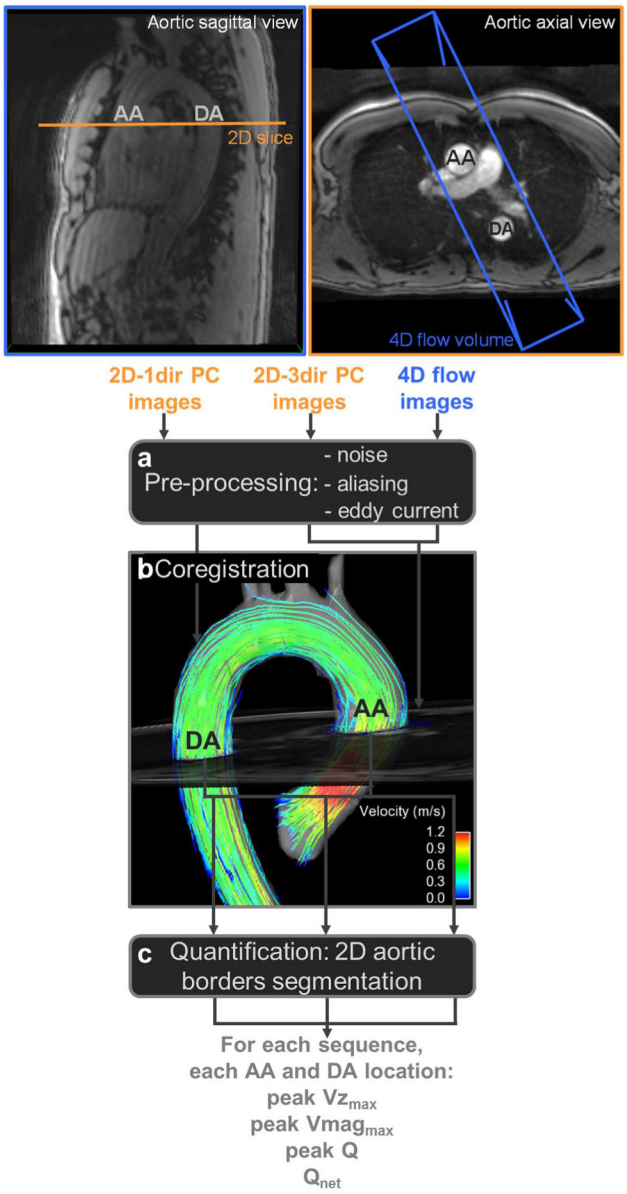

Fig. 1.

Analysis workflow of 2D one-directional (2D-1dir), three-directional (2D-3dir) and 4D flow phase-contrast (PC) MRI data: preprocessing (**a**), coregistration of the 2D slice location on 4D flow data (**b**), as well as 2D segmentation of ascending (AA) and descending (DA) aortic borders (**c**), used for the estimation of peak through-plane velocity (peak Vz_{max}), peak velocity magnitude (peak $Vmag_{max}$), peak flow (peak Q) and net flow volume (Q_{net})

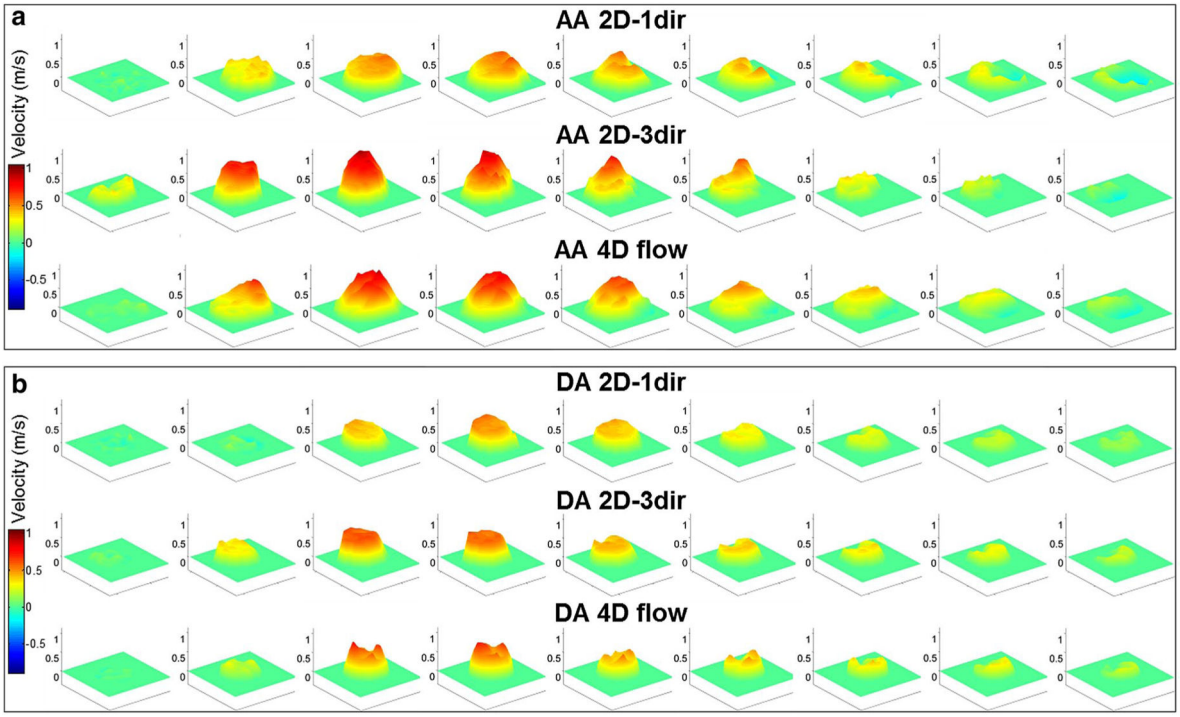

Fig. 2.

Examples of velocity profiles obtained in the AA (**a**) and DA (**b**) using 2D-1dir (*top row*), 2D-3dir (*middle row*) PC-MRI and 4D flow (*bottom row*) data throughout the systolic period in a healthy volunteer

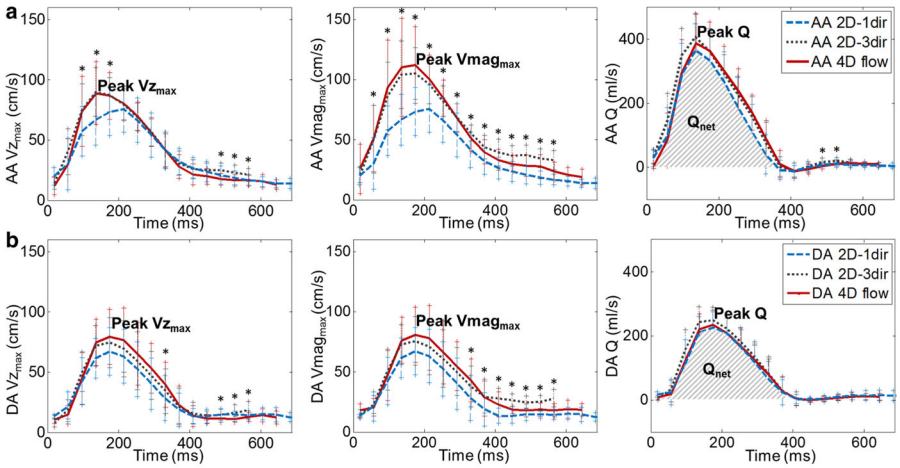

Fig. 3.

Group-averaged maximal through-plane velocity Vz_{max} (*left*), maximal velocity magnitude $Vmag_{max}$ (*middle*) and flow rate Q (*right*) throughout the cardiac cycle as estimated in the AA (**a**) and DA (**b**), using 2D-1dir (*dashed blue lines*), 2D-3dir (*dotted grey lines*) PC-MRI and 4D flow (*solid red lines*) data. Standard deviations over the whole group are represented as *bars* for each cardiac phase. *Indicates $p < 0.05$ for comparison across the three sequences

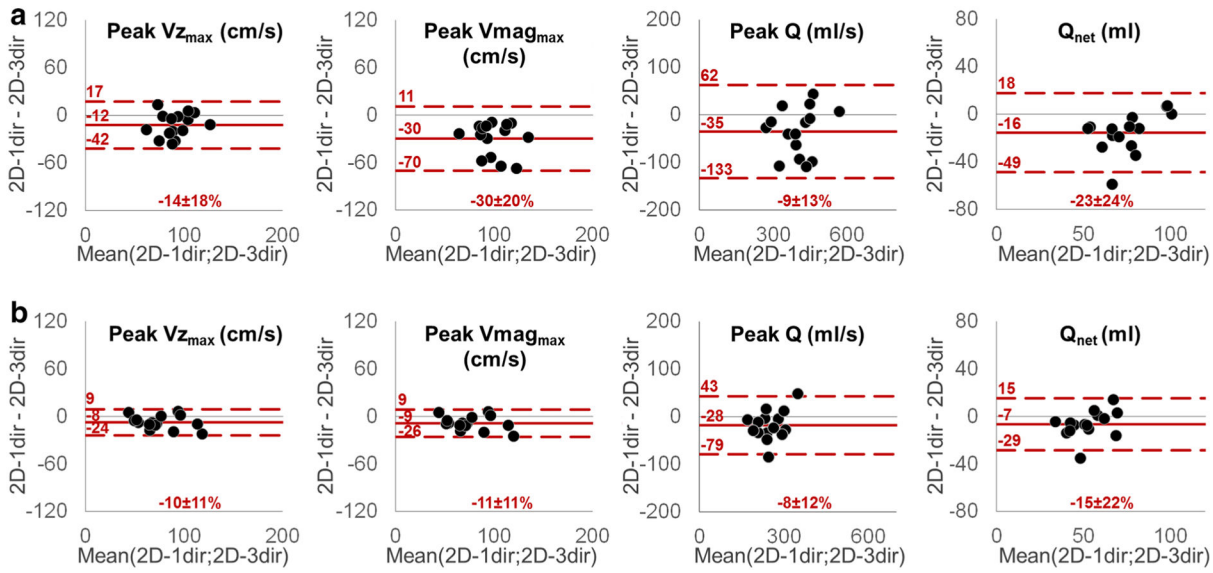

Fig. 4.

Bland–Altman diagrams for comparison between 2D-1dir and 2D-3dir PC-MRI peak systolic maximal through-plane velocity (peak Vz_{max}), peak systolic maximal velocity magnitude (peak $Vmag_{max}$), peak systolic flow (peak Q) and net flow volume (Q_{net}), in the AA (**a**) and DA (**b**). *Solid red line* indicates mean bias while *dashed red lines* indicate limits of agreement. Mean values of the relative difference in percentage of the averaged value are provided

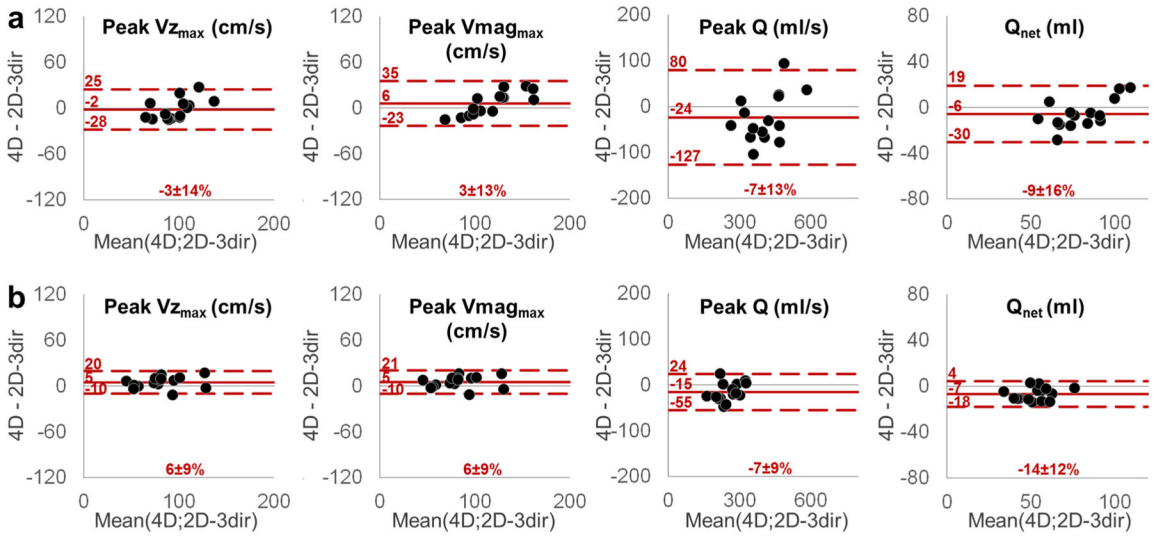

Fig. 5.

Bland–Altman diagrams for comparison between 2D-3dir PC-MRI and 4D flow peak through-plane velocity (peak Vz_{max}), peak velocity magnitude (peak $Vmag_{max}$), peak flow (peak Q) and net flow volume (Q_{net}), in the AA (**a**) and DA (**b**). *Solid red line* indicates mean bias while *dashed red lines* indicate limits of agreement. Mean values of the relative difference in percentage of the averaged value are provided

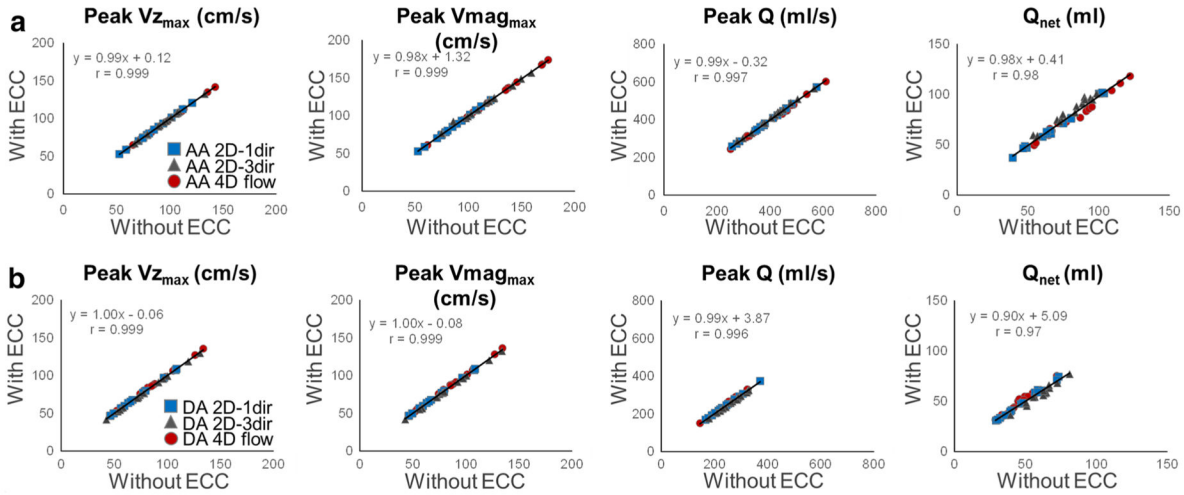

Fig. 6.

Linear regressions for comparison between peak through-plane velocity (peak Vz_{max}), peak velocity magnitude (peak $Vmag_{max}$), peak flow (peak Q) and net flow volume (Q_{net}), in the AA (**a**) and DA (**b**) estimated with and without performing eddy current correction (ECC), while pooling the three PC-MRI sequences. Slopes and Pearson correlation coefficients (r) are provided

Table 1

Acquisition parameters used for each of the 2D-1dir, 2D-3dir PC-MRI and 4D flow sequences

	BH/FB	TR (ms)	TE (ms)	FA (°)	AM	SRes (mm^3)	NSeg	Time frames (n)	TRes (ms)	Venc (cm/s)	rBW (Hz/pixel)	Scan time
2D-1dir	BH	5	2.4	20	192 × 99–131	1.8–1.9 × 2.1–2.5 × 6	4	13–31	39.2	150	500	20–30 s
2D-3dir	FB	4.8	2.5	20	192 × 108–140	1.8–1.9 × 2.4–2.6 × 6	2	16–27	38.4	150	450	1–2 min
4D flow	FB	4.9	2.5	7	160 × 88–104	3.0–3.4 × 2.3–2.5 × 2.5–2.7	2	17–30	39.2	150	445	7–13 min

BH/*FB* breath-holding or free breathing, *TR* repetition time, *TE* echo time, *FA* flip angle, *AM* acquisition matrix, *SRres* spatial resolution, *NSeg* number of segments, *TRes* acquired temporal resolution, *Venc* encoding velocity, *rBW* receiver bandwidth, *2D-1dir* 2D one-directional PC-MRI, *2D-3dir* 2D three-directional PC-MRI

Table 2

AA and DA peak Vz_{max}, $Vmag_{max}$ and Q, Q_{net} and systolic area mean values

Location	Sequence	Peak Vz_{max} (cm/s)	Peak $Vmag_{max}$ (cm/s)	Peak Q (ml/s)	Q_{net} (ml)	Systolic area (mm^2)
AA	2D-1dir	85 ± 19 *	85 ± 19 *	384 ± 85 *	68 ± 21 *	866 ± 247 *
	2D-3dir	97 ± 17	115 ± 22	420 ± 76	83 ± 13	976 ± 234
	4D flow	96 ± 24	121 ± 34	396 ± 99	77 ± 21	944 ± 255
DA	2D-1dir	72 ± 22 *	72 ± 22 *	243 ± 55 *	49 ± 14 *	482 ± 137 *
	2D-3dir	79 ± 24	80 ± 25	261 ± 45	56 ± 10	502 ± 138
	4D flow	84 ± 26	85 ± 26	245 ± 52	49 ± 12	505 ± 122

Peak Vz_{max} peak through-plane velocity, *peak* $Vmag_{max}$ peak velocity magnitude, *peak Q* peak flow, Q_{net} net volume, *AA* ascending aorta, *DA* descending aorta, *2D-1dir* 2D one-directional PC-MRI, *2D-3dir* 2D three-directional PC-MRI

* Indicates $p < 0.05$ between 2D-1dir and 2D-3dir

Table 3

Bland–Altman analysis for comparison between indices estimated with and without performing eddy current correction

Location and index	2D-1dir	2D-3dir	4D flow
Bias [limits of agreement]	With-without eddy current correction		
AA			
Peak Vz_{max} (cm/s)	0.31 [−0.84; 0.22]	0.41 [−0.27; 1.10]	0.85 [−1.94; 0.24]
Peak $Vmag_{max}$ (cm/s)	0.31 [−0.84; 0.22]	0.05 [−4.10; 4.00]	0.91 [−1.82; 0.01]
Peak Q (ml/s)	2.79 [−7.35; 1.78]	4.19 [−2.99; 11.4]	7.73 [−17.5; 2.00]
Q_{net} (ml)	2.18 [−5.80; 1.43]	2.99 [−1.86; 7.84]	4.89 [−10.4; 0.58]
DA			
Peak Vz_{max} (cm/s)	0.15 [−0.37; 0.67]	0.99 [−1.75; −0.22]	0.95 [−0.49; 2.39]
Peak $Vmag_{max}$ (cm/s)	0.15 [−0.37; 0.67]	1.19 [−2.39; 0.01]	0.93 [−0.47; 2.33]
Peak Q (ml/s)	0.73 [−1.84; 3.29]	4.79 [−9.60; 0.02]	4.63 [−1.86; 11.1]
Q_{net} (ml)	0.53 [−1.59; 2.65]	3.69 [−7.32; −0.06]	2.70 [−0.87; 6.26]

Means bias and limits of agreement (in brackets) are provided

2D-1dir 2D one-directional PC-MRI, *2D-3dir* 2D three-directional PC-MRI, *peak* Vz_{max} peak through-plane velocity, *peak* $Vmag_{max}$ peak velocity magnitude, *peak Q* peak flow, Q_{net} net volume, *AA* ascending aorta, *DA* descending aort

Table 4

Previous comparisons in the literature between aortic 2D PC-MRI and 4D flow in healthy populations

Studied population	MRI acquisitions	Reported findings
Stalder, MRM2008 [19]		
n = 19	3T	4D flow AA peak Q slightly lower than 2D-3dir
Mean age 23 [20–34] years	2D-3dir: SR = 1.24–1.82 × 1.25–1.82 × 5 mm^3	AA 2D-3dir Q_{net} = 74.4 ± 16.2 ml
	TRes = 24.4 ms, 28–40 cardiac phases	AA 4D flow Q_{net} = 73.9 ± 18.9 ml
	FB with navigator, prospective gating	DA 2D-3dir Q_{net} = 61.6 ± 13.0 ml
	4D flow: SR = 2.71–2.93 × 1.58–1.69 × 2.6–3.5 mm^3	DA 4D flow Q_{net} = 45.4 ± 11.7 ml
	13–15 cardiac phases	Mean absolute difference 2D-3dir − 4D flow Q_{net} (8 aortic locations) = 8.88 ± 7.02 ml
	FB, prospective gating	Median relative error 2D-3dir − 4D flow Q_{net} (8 aortic locations) ~12 %
Brix, JCMR2009 [13]		
n = 9	1.5T	AA 2D-1dir Q_{net} = 89.5 ± 13.5 ml
Mean age 29 ± 7 years	2D-1dir: SR = 1.41 × 1.41 × 5 mm^3, TRes = 36 ± 9 ms	AA 4D flow Q_{net} = 92.7 ± 17.5 ml
	29.7 ± 3.7 cardiac phases, FB with navigator, prospective gating	Mean absolute difference 4D flow − 2D-1dir AA Q_{net} = 4.0 ± 8.8 ml
	4D flow: SR = 3 × 3 × 3 mm^3, TRes = 55 ± 12 ms	No statistical diffences between 2D-1dir and 4D flow AA Q_{net} (p = 0.68)
	20 cardiac phases, FB with navigator, prospective gating	
Hope, JMRI2010 [24]		
n = 8	1.5T	No comparison between 2D and 4D flow reported in healthy volunteers, only vs. patients with aortic coarctation
Mean age 30.8 ± 5.2 years	2D-1dir: slice thickness = 8 mm, BH	
	4D flow: SR = 1.17 × 1.56 × 2.6 mm^3, TRes = 74–77 ms	
	FB with bellows, retrospective gating	
Carlsson, JCMR2011 [14]		
n = 13	1.5T	4D flow AA and MPA peak Q significantly lower than 2D-1dir
Mean age 32 ± 12 years	2D-1dir: SR = 1.2 × 1.2 × 6 mm^3	Mean relative error 2D-1dir − 4D flow AA and MPA Q_{net} = −3.6 ± 14.8 % (NS)
	35 cardiac phases, FB with no navigator, retrospective gating	
	4D flow: SR = 3 × 3 × 3 mm^3, TRes = 50–55 ms	
	40 cardiac phases, FB with navigator, retrospective gating	
Valverde, JCMR2012 [23]		
	1.5T	No comparison between 2D and 4D flow reported in healthy volunteers, only vs. patients with single-ventricle physiology
	2D-1dir: SR = 1.2 × 1.2 × 7 mm^3, 35–40 cardiac phases	

Studied population	MRI acquisitions	Reported findings
	FB with no navigator, retrospective gating	
	4D flow: 1.5 × 1.5 × 2.3 mm^3, 22–25 cardiac phases	
	FB with no navigator, retrospective gating	
Nordmeyer, JMRI2013 [18]		
n = 7	3T	Mean absolute error 2D-1dir − 4D flow AA and MPA V_{max} = 10 % (NS)
Mean age 34 ± 7 years	2D-1dir: SR = 1.1–2.2 × 1.1–2.2 × 7 mm^3	AA 2D-1dir Q_{net} = 89 ± 10 ml
	35 cardiac phases, FB, retrospective gating	AA 4D flow Q_{net} = 88 ± 10 ml
	4D flow: SR = 1.5–2.1 × 1.5–2 × 2.5 mm^3	Good agreement between 2D-1dir and 4D flow AA and MPA Q_{net}
	24 cardiac phases, FB with no navigator, retrospective gating	
Frydrychowicz, InvestRadiol2013 [16]		
n = 18	3T	AA 2D-1dir Q_{net} = 100.6 ± 27.8 ml
Mean age 41.6 ± 16.21 [22.5–73.5] years	2D-1dir: SR = 1.45 × 1.45 × 7 mm^3	AA 4D flow Q_{net} = 95.9 ± 19.1 ml
	19.7 ± 4.7 [13–37] cardiac phases, BH, prospective gating	Mean relative difference 2D-1dir − 4D flow AA Q_{net} = −12.0 ± 24.1 ml
	4D flow: SR = 1.4 × 1.4 × 1.4 mm^3	
	24 cardiac phases, FB with bellows, retrospective gating	
Current study		
n = 15	1.5T	AA 2D-1dir Q_{net} = 68 ± 21 ml/DA 2D-1dir Q_{net} = 49 ± 14 ml
Mean age 51 ± 18 [19–78] years	2D-1dir: SR = 1.8–1.9 × 2.1–2.5 × 6 mm^3, TRes = 39.2 ms	AA 2D-3dir Q_{net} = 83 ± 13 ml/DA 2D-1dir Q_{net} = 56 ± 10 ml
	[13–31] cardiac phases, BH, prospective gating	AA 4D flow Q_{net} = 77 ± 21 ml/DA 4D flow Q_{net} = 49 ± 12 ml
	2D-3dir: SR = 1.8–1.9 × 2.4–2.6 × 6 mm^3, TRes = 38.4 ms	2D-1dir AA and DA Q_{net} significantly lower than 2D-3dir
	[16–27] cardiac phases, FB with navigator, prospective gating	Good agreement between 2D-3dir and 4D flow AA and DA Q_{net}
	4D flow: SR = 3.0–3.4 × 2.3–2.5 × 2.5–2.7 mm^3, TRes = 39.2 ms	Mean absolute/relative difference 2D-1dir − 2D-3dir AA Q_{net} = −16 ml/−23 ± 24 %
	[17–30] cardiac phases, FB with navigator, prospective gating	Mean absolute/relative difference 2D-1dir − 2D-3dir DA Q_{net} = −7 ml/−15 ± 22 %
		Mean absolute/relative difference 4D − 2D-3dir AA Q_{net} = −6 ml/−9 ± 16 %
		Mean absolute/relative difference 4D − 2D-3dir DA Q_{net} = −7 ml/−14 ± 12 %

SR spatial resolution, *TRes* acquired temporal resolution, *FB* free breathing, *MPA* main pulmonary artery, *NS* non-significant difference, *BH* breath-holding